Resonant ir laser stimulation of the desorption of methanol adsorbed on Cu(110)

A. Peremans
Laboratoire de Spectroscopie Moléculaire de Surface, Institute for Studies in Interface Sciences (I.S.I.S.), Facultés Universitaires Notre Dame de la Paix, rue de Bruxelles 61, B-5000 Namur, Belgium

A. Dereux
Laboratoire de Physique du Solide, Institute for Studies in Interface Sciences (I.S.I.S.), Facultés Universitaires Notre Dame de la Paix, rue de Bruxelles 61, B-5000 Namur, Belgium

F. Maseri, J. Darville, and J-M. Gilles
Laboratoire de Spectroscopie Moléculaire de Surface, Institute for Studies in Interface Sciences (I.S.I.S.), Facultés Universitaires Notre Dame de la Paix, rue de Bruxelles 61, B-5000 Namur, Belgium

J-P. Vigneron
Laboratoire de Physique du Solide, Institute for Studies in Interface Sciences (I.S.I.S.), Facultés Universitaires Notre Dame de la Paix, rue de Bruxelles 61, B-5000 Namur, Belgium
(Received 12 July 1991)

The reactive system $CH_3OH/Cu(110)$ has been characterized by thermal desorption and infrared reflection-absorption spectroscopies. This provides the knowledge of the reactive system properties necessary for the interpretation of the ir photodesorption experimental results. These properties are the sticking coefficient of methanol on Cu(110) at 90 K, the monolayer density, the ir absorbance, and the structure of the adsorbate. In particular, ir spectroscopy demonstrates the possibility of thermally activating the crystallization of the amorphous adsorbate obtained upon condensation on Cu(110) at 90 K. The experimental setup used for the measurements of the photodesorption yield (Y_{PD}) makes use of an optical parametric oscillator generating ir pulses about 15 ns long and frequencies tunable from 2800 to 3450 $cm.^{-1}$ This frequency range includes the ir bands corresponding to the asymmetric methyl and hydroxyl stretching modes. The ir Y_{PD} of amorphous and crystallized films have been measured as a function of the laser-beam frequency and fluence, of the substrate coverage, and of the temperature (from 90 to 120 K). The correspondence between the Y_{PD} spectra and the ir spectrum of liquid methanol indicates the occurrence of adsorbate melting during the photodesorption process. The saturable exponential evolution of the Y_{PD} as a function of the laser fluence reveals the thermal nature of the process. The Y_{PD} of the amorphous methanol thin films increases greatly upon their crystallization. This is tentatively explained as a consequence of a change in the film morphology. These experimental results are interpreted quantitatively in the framework of the thermal photodesorption mechanism due to the resonant substrate heating.

I. INTRODUCTION

Since the development of lasers generating frequency-tunable ir pulses, increasing effort has been devoted to the study of surface-process stimulation by resonant excitation of vibrations of the molecules in the gaseous or in the adsorbed phase.[1-3] This offers the possibility of investigating the relevance of specific molecular vibration excitation for overstepping the activation barrier of a surface reaction. An interesting prospect for such investigations would be the photostimulation of isotopically or chemically selective surface processes.

It has been demonstrated that the resonant ir excitation of molecules in the gas phase may decrease their physisorption probability onto a cooled wall,[4] increase the yield of a reaction catalyzed by a metallic surface,[5] or generate highly reactive fragments for a subsequent surface reaction.[6] Except in the case of SF_6/Si, where the resonant excitation of the adsorbate by a CO_2 laser activates the etching of the surface,[7] the spectroscopic (frequency-dependent) investigations on a surface-process stimulation by ir laser irradiation of the adsorbed phase have been restricted to the photodesorption process.[8] The reports concerning this research theme appeared in the literature at the beginning of the 1980s. The possibility of observing the resonant character of the ir photodesorption process has been demonstrated for molecules adsorbed on monocrystalline or polycrystalline metallic or insulating substrates.[9-25] The reactive systems selected for these investigations are listed in Table I. We generally speak of *photodesorption* for adsorbate thicknesses ranging from 1 monolayer (ML) to a few tens of monolayers such that the process efficiency is substrate and coverage dependent. Resonant ir *photoablation* of thick adsorbates,[29-35] which is substrate independent, is also reported in Table I. In all cases, the resonant structure of the photodesorption-yield (Y_{PD}) spectra could be assigned to the resonant excitation of an adsorbate vibra-

tional mode. All these experiments were performed using a pulsed laser beam in order to obtain a high instantaneous irradiance. The photodesorption of CO from NaCl(100) irradiated by a cw CO laser ($\approx$2100 cm^{-1}) turned out to be unobservable.[36] The other important features common to the majority of the investigations are a supralinear dependence of Y_{PD} versus the laser fluence,[9-11,13,20,21,23-25] an increase of Y_{PD} with increasing coverage values,[12,13,17,20,23-25,33] and a lack of isotopic selectivity [NH_3-ND_3/Cu(100) or Ag film,[24] $^{12}C^{16}O$-$^{13}C^{16}O$/NaCl film,[15,16] C_4D_{10}-C_4H_{10}/$Al_2O_3(11\bar{2}0)$,[17] and C_5H_5N-C_5D_5N/KCl film[9]]. Selective ir photodesorption of CH_3F when coadsorbed with another chemical species has been achieved in the cases of CH_3F-CH_2F_6/NaCl film[37] and CH_3F-CO/Cu.[38] For the latter experiments, it was not established whether the chemical selectivity was a consequence of the ir laser-excitation selectivity or of the difference in desorption kinetics between the two coadsorbed species. Efforts were also devoted to the measurement of the photodesorbed molecule speed distribution.[19,24,30,39] For substrates showing a high specific surface like condensed films,[11,13,15,19] or in the case of thick adsorbed films,[27,33] the adsorbate ir spectrum could be recorded and compared with the Y_{PD} spectra.

Considerable theoretical efforts have also been made to

TABLE I. Reactive systems selected for performing resonant ir photodesorption experiments.

Adsorbate	Substrate	Substrate temperature (K)	Laser type[a]	Frequency (cm^1)	References
Insulating substrates					
C_5D_5N	KCl	95	CO_2	970	9
C_5H_5N	KCl	95	CO_2	1033	10
CH_3F	film NaCl	77	CO_2	975	11–13
CH_3F	NaCl(100)	64	CO_2	975	13,14
CO	film NaCl	80	$CO_2\times2$	2110	15,16
C_4H_{10}	$Al_2O_3(11\bar{2}0)$	90	FEL	3000	17,18
C_2H_4	film NaCl	81,35	CO_2	970	19
C_2H_4	NaCl(100)	45	CO_2 (1970)	970	19
NH_3	film NaCl	90	freq. diff.	3370	20
Metallic substrates					
C_6H_5N	Ag(110)	95	CO_2	1033	9
C_6H_5N	film Ag	95	CO_2	1033	21,22
NH_3	Cu(100)	90	freq. diff.	3350	23–25
ND_3	Cu(100)	90	freq. diff.	2500	23–25
NH_3/1Mc	film Ag	60,10	freq. diff.	3340	23–25
Xe and NH_3	film Ag	12	freq. diff.	3400	20
Photoablation of thick adsorbates					
SF_6		$\approx$67	CO_2	950	26
CCl_4		$\approx$77	CO_2	980	27,28
$C_6H_{10}Cl_2$		$\approx$77	CO_2	980	29–31
D_2O		$\approx$77	CO_2	1048	28
CH_3F		$\approx$77	CO_2	983	28
CH_3OH		$\approx$77	CO_2	1048	28
C_6H_5CO		$\approx$77	CO_2	1073	28
CH_2ClCH_2Cl		$\approx$77	CO_2	946	32
$C_6H_5CF_3$		77	CO_2	1070	33,34
NO		13	$CO_2\times2$	1870	33
$C_6H_4F_2$		77	CO_2	1085	34
C_6H_6		$\approx$77	CO_2	1035	35

[a]Freq. diff. denotes frequency difference between a dye and doubled Nd:YAG laser beams; FEL denotes free-electron laser; $\times2$ denotes frequency-doubled beam.

predict or to interpret these experimental results. Mathematical formalisms allowing the description of the photostimulation of adatom migration[40] or desorption,[41] and of the resonant substrate heating,[42] when the ir laser beam is coupled with the adbond, have been detailed. Photodesorption mechanisms corresponding to the experimental situation where the ir laser beam excites an internal vibrational mode of the admolecule, have also been studied. Hussla *et al.*,[24] followed by some of us,[43] proposed that the photodesorption of NH_3 from Cu(100) may be due to fast relaxation, towards the substrate, of the energy resonantly absorbed by the adsorbate, which causes the so-called *resonant heating* of the substrate subsurface region. In that case, the effective charge of the excited internal vibration had to be adjusted to a value one order of magnitude above its actual gas-phase value, in order to explain the efficiency of the process. This leads to an adsorbate ir absorbance, two orders of magnitude higher than that extrapolated from the gas-phase value, and obviously renders this interpretation[24,43] questionable. Lucas *et al.*[44] have suggested that photodesorption can occur by *elastic tunneling* from a vibrationally excited molecular state to a desorption state of the adbond continuum, but they have also demonstrated that this photodesorption channel was not significant in the case of CO/NaCl (Ref. 36) when irradiated by a cw CO laser. Kreuzer *et al.*[45] proposed that this *tunneling may inelastically* occur by simultaneous emission or absorption of a substrate phonon. Gortel *et al.*[46] evaluated the transfer rate of the vibrational energy from the excited internal vibration, through the adbond and to the substrate phonons, due to the anharmonicity of the interatomic potentials. They proposed that photodesorption can occur by *accumulation of the energy in the adbond vibration.* In the case of CH_3F/NaCl, the theoretically estimated fluence that causes a detectable Y_{PD} was four orders of magnitude smaller than that used to perform the experiment. Fain *et al.*[47] suggested that photodesorption can occur by *destabilization of a substrate surface vibrational mode.* Ephrain *et al.*[48] also studied the relevance of the admolecule frustrated rotations in the photodesorption process. The influence of the excited vibrational mode anharmonicity[49,50] of the homogeneous and inhomogeneous broadenings[51] of the corresponding ir-absorption band have also been investigated. Although it was shown that the lateral interactions between local adsorbate vibrations (V-V interactions) may restore efficient pumping of the molecular vibration[52] by overcoming the anharmonicity of the latter, the nature of these V-V interactions has not been not determined. In a previous work,[53] we demonstrated that the direct dipolar coupling is not responsible for the lack of isotropic selectivity in the photodesorption of $^{12}C^{16}O$-$^{13}C^{16}O$/NaCl. Fain *et al.*[54] showed that the interactions between the continuum and the bond states of neighboring-molecule adbonds could only partly explain the lack of isotopic selectivity, in the case of NH_3-ND_3/Cu(100).

Clearly, although considerable experimental work has been performed in order to characterize the ir photodesorption process, and in spite of the numerous theoretical investigations of various ir photodesorption mechanisms, no quantitative agreement has ever been achieved between experimental and theoretical results. The mechanism of the photodesorption process, as well as the efficiency of the V-V interactions within the adsorbate, remain questionable.

In this work, we present the results of the photodesorption of methanol adsorbed on Cu(110) by resonantly exciting its two highest-frequency vibrational modes, namely asymmetric methyl and hydroxyl stretching. The frequencies of both vibrations are close to 3000 cm^{-1}. The energy of the corresponding vibrational quanta lies near 36 kJ/mol, which is comparable to the physisorption energy of methanol, namely $\sim$40 kJ/mol. This was an *a priori* intuitive criterion indicating the feasibility of the photodesorption experiment. The copper substrate has been selected because of its good ir reflectivity and its high thermal conductivity, both of which minimize direct substrate heating due to the partial absorption of the ir laser beam by the copper surface. This direct substrate heating induces undesired nonresonant thermal desorption of the adsorbate.

In Sec. III we present a summary of the characterization of this reactive system by thermal desorption (TDS) and infrared reflection-absorption spectroscopies (IRAS). Particular attention was paid to the absolute determination of some physical properties of the system, such as the monolayer density and the adsorbate ir absorbance. In Sec. IV we present the experimental results of the ir photodesorption experiment. The evolution of Y_{PD} has been systematically measured as a function of the modifiable experimental parameters: laser-beam frequency and fluence, substrate coverage and temperature, amorphous or crystallized adsorbate. These results are interpreted quantitatively in Sec. V in the framework of the photodesorption mechanism due to *resonant heating* of the substrate. The agreement between experiment and theory will appear to be much better than that usually attained in this field.

II. EXPERIMENT

The 12-mm-diam (110) copper disk was mechanically polished and cleaned under ultrahigh-vacuum conditions (base pressure $<1\times10^{-10}$ Torr) by cycles of Ar^+-ion bombardment (0.5 keV, 5 $\mu A/cm^2$, 20 min) followed by 3-min-long anneal at 1000 K. The sample cleanliness was considered satisfactory when the surface contamination level, mainly due to sulfur migrating from the bulk, was below the detection limit of our four-grid-analyzer Auger spectrometer. Well-defined, low-energy electron-diffraction patterns demonstrated the crystallographic quality of the surface. The sample was maintained by four lateral screws on a liquid-nitrogen-cooled sample holder. The sample could be heated by electronic bombardment and its temperature was measured with a Chromel-Alumel thermocouple pressed against its side by a stainless-steel spring. The sample surface normal was brought in a line-of-sight arrangement along the axis of a quadrupole-mass spectrometer when performing TDS or Y_{PD} measurements. The mass spectrometer was provided with a copper shield in order to select geometrically

the molecules desorbing from the sample surface.

The ir laser pulses used for the photodesorption experiment are generated by an optical parametric oscillator (OPO). Our OPO is a prototype developed by the SOPRA company (Bois-Colombes, France;[55] the statement in Ref. 55 that the idler pulse duration was measured with an InSb detector is erroneous). The idler beam of the OPO is frequency tunable from 2800 to 3450 cm^{-1}. The pulse energy reaches the value of 10 mJ at the center of the tuning range, which is remarkable, being one order of magnitude higher than that provided by commercialized systems at the beginning of our measurements (Datachrome system by Quantel or Wex-1 by Spectra Physics). The OPO is pumped by a Nd-YAG (yttrium-aluminum-garnet) laser (Quantel) generating 20-ns-long [full width at half maximum (FWHM)] pulses. The duration of the idler pulses, used to perform the photodesorption experiment, may be estimated to be 15 ± 5 ns (FWHM). A 2-mm-diam diaphragm is used to select an homogeneous part of the beam. Then the beam passes through an adjustable attenuator made of rotatable reflecting CaF_2 plates and is focused on the sample by a 350-mm-focal-length CaF_2 lens. The incidence angle is 73°. The surface of the elliptic beam spot is 0.1 mm^2. The pulse energy is measured using a pyroelectric detector that collects the beam reflected by one of the CaF_2 attenuator plates. The *p*-polarized component of the ir beam incident on the sample contains $90\pm5\%$ of the pulse energy. The sample is slightly displaced laterally after each ir laser-pulse emission in order to present always a virgin adsorbate to the next laser pulse. Y_{PD} is determined by counting the molecules detected by the mass spectrometer (tuned on mass 31 for the detection of the electron-impact CH_3O^+ fragment of methanol) during a 22-ms window synchronized with the laser-pulse emission. The dynamical range of the Y_{PD} measurement extends over more than five orders of magnitude. The results presented in Sec. IV were averaged over 10 laser pulses.

The sample may finally be brought into the path of the beam emerging from an ir reflection-absorption spectrometer, at an incidence of ~84°. This spectrometer, working in high-vacuum conditions, fitted with a new ir source made of a tantalum cavity heated at 2500 K and with a photoelastic modulator-based detection technique, has been described elsewhere.[56]

The copper sample was exposed to methanol through a retractable capillary array doser that can be brought within 2 mm of the surface. All exposures were performed while the sample was cooled at 90 K. The exposure values were absolutely determined by measuring the pressure drop inside the reservoir feeding the doser.

III. CHARACTERIZATION OF THE REACTIVE SYSTEM

The evolution of the TDS spectra of methanol versus increasing exposure values is presented in Fig. 1. The two desorption peaks *C* and *P* are assigned in accordance with previous investigations on this reactive system.[57–59] The broad peak *C* centered at 180 K corresponds to the

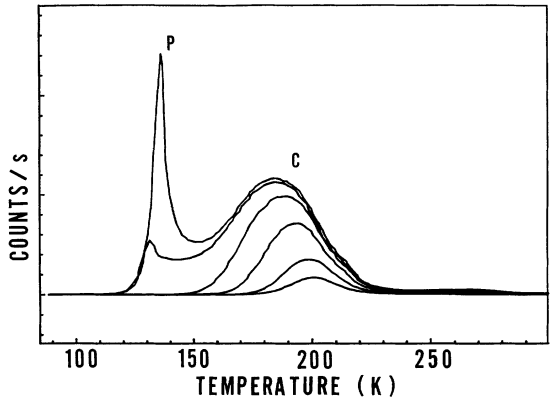

FIG. 1. TDS spectra of CH_3OH adsorbed on Cu(110) at 90 K for increasing exposure values: 0.3, 0.5, 0.8, 1.1, 1.6, and 1.9 L.

desorption of molecules from the first monolayer. This peak saturates at an exposure value of 1.6 L (1 L = 1 langmuir = 10^{-6} Torr s). Exposures higher than this threshold induce the appearance of a second and thinner peak (*P* in Fig. 1) centered at 145 K. The latter peak is not saturable and corresponds to the desorption of the molecules physisorbed in the multilayer phase. As demonstrated in our previous works,[55,59] the decomposition of methanol on the clean Cu(110) surface is negligible, and the sticking coefficient of methanol on that surface cooled at 90 K is equal to that from the submonolayer to the multilayer level. The monolayer density may therefore be derived from the exposure threshold value of 1.6 L, and is equal to one molecule per ~16 $Å^2$. The correspondence between that value and the density of the molecular planes of the methanol crystal, which contain the hydroxyl-group axis,[60] indicates that this monolayer density is stereometrically limited.

Because Sec. IV will concentrate on the ir photodesorption of physisorbed molecules, particular attention was devoted to the study of the desorption kinetics of the multilayer phase. The desorption spectra of thick adsorbates, for two coverage values and three heating rates varying over two orders of magnitude, are presented in Fig. 2. The experimental curves can be reproduced theoretically assuming a zeroth-order desorption kinetics given by the following equation:

$$\frac{d\Theta}{dt}=S(\Theta)Ae^{-(E_a/RT)}, \tag{1}$$

where Θ is the coverage expressed in ML. *R* and *T* are the gas constant and the substrate temperature, respectively. *A* and E_a are the frequency factor and the activation energy for desorption, respectively. $S(\Theta)$ is the step function equal to 1 for $\Theta>0$ and 0 for $\Theta\leq 0$.

Assuming the pumping speed of methanol to be infinite, the mass-spectrometer signal would be proportional to $d\Theta/dT$ and exhibit an exponential increase given by (1) terminated by a vertical falling edge corresponding to the depopulation of the adsorbate. As observed in Fig. 2, the falling edges of the measured desorp-

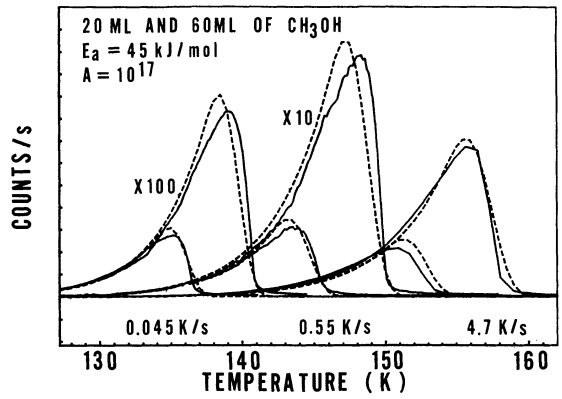

FIG. 2. TDS spectra of the physisorbed phase recorded at three heating rates and two coverage values. Solid line, experimental spectra; dashed line, simulated spectra. The spectra recorded at the low heating rates of 0.045 and 0.55 K/s have been multiplied by a factor of 100 and 10, respectively.

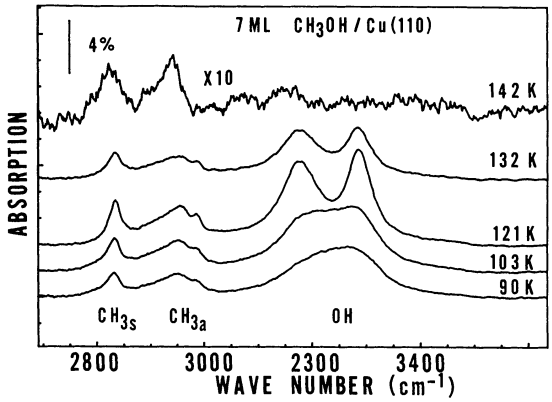

FIG. 3. Evolution of the IRAS spectra of a methanol film as a function of successive 2-min anneal at increasing temperatures (resolution 10 cm^{-1} FWHM).

tion traces are smoother than expected. This may be attributed to the fact that the multilayer adsorbate is gradually sprinkled with holes as the coverage decreases below the adsorbate corrugation thickness, or may also be explained if we consider that not only does the adsorbate upper layer contribute to $d\Theta/dt$ but so do the underlying ones. In both cases, the desorption kinetics may better be described by replacing the step function $S(\Theta)$ by a smoother one $[S'(\Theta)]$ that gradually decreases from 1 to 0 when Θ goes below a critical coverage (C_c) to 0 and behaves as $S(\Theta)$ elsewhere. Finally, we cannot discard the facts that a temperature inhomogeneity of a few degrees across the sample, or the finite methanol pumping speed, contributes to the smoothing of the measured desorption traces. For the purpose of determining the desorption kinetic parameters (A,E_a), we performed a simulation using (1) and replacing $S(\Theta)$ by $S'(\Theta)$, which decreases following a second-order law, $2\Theta/C_t - (\Theta/C_t)^2$, when $\Theta < C_t$. C_t was adjusted to 30 and 10 ML for the 60- and 20-ML spectra, respectively. The simulated curves were scaled in order to make their surfaces correspond to the experimental ones. The best fit was obtained for $A = 10^{17}$ and $E_a = 45$ kJ/mol. Besides allowing an accurate determination of the desorption-kinetic parameters of the physisorbed layer, these measurements also demonstrate their invariability for a range of heating rates accessible by TDS and varying over two orders of magnitude.

IRAS spectra of 7 ML of methanol condensed on Cu(110) are presented in Fig. 3. The first curve (90 K) was recorded immediately after the condensation of methanol on the substrate cooled at 90 K. The three absorption bands that are clearly detected correspond to the three highest-frequency fundamental vibrations of methanol. According to previous investigations of the ir properties of methanol in the gaseous, liquid, and solid phases,[61,62] or adsorbed on Pt(111) (Ref. 63) and Cu(111),[64] the bands situated at 2830 and 3280 cm^{-1} correspond to symmetric methyl (CH_{3s}) and hydroxyl (OH) stretching, respectively. The central band at 2945 cm^{-1} receives a contribution from the two nearly degenerate asymmetric methyl stretchings (CH_{3a}) and from the second harmonic of the methyl-group deformation. Annealing the substrate at about 121 K for 2 min optimizes the splitting of the OH band into two components. This testifies to the film crystallization. The two components are assigned to the in-phase $(OH)_{ip}$ and out-of-phase $(OH)_{op}$ vibrations of the hydroxyl group of the methanol molecules in the molecular chains of the crystal.[61,62,65] Annealing at temperatures above 121 K induces the attenuation of the ir spectra as a consequence of the multilayer phase desorption. That desorption is complete after annealing at 142 K, and we are then left with the ir spectrum of the first methanol monolayer, which is characterized by the absence of the OH band. This absence was interpreted in our previous work[59] as the consequence of the orientation of the hydroxyl-group axis parallel to the metallic surface. This particular orientation of the methanol molecules in the annealed first monolayer renders the OH vibration undetectable under the selection rules of IRAS.[66]

The ir spectra presented in Fig. 3 allow the determination of the effective absorption coefficient of the methanol adsorbate. In particular, the intensity of the CH_{3a} band increases from 2% to 3% as the 7 ML of amorphous methanol crystallize. This intensity varies, therefore, from 0.3% to 0.45% per adsorbed monolayer. We refer to our previous work[59] (the ir absorbances reported in Ref. 59 have been underestimated by a factor of 2) for a more detailed characterization by IRAS of the CH_3OH/Cu(110) system, at submonolayer and multilayer levels.

IV. ir PHOTODESORPTION EXPERIMENT

The Y_{PD} spectrum of a 200-ML-thick amorphous methanol film condensed at 90 K is presented in Fig. 4. Two resonant structures clearly appear and their positions are compared with those of the ir absorption bands of methanol in gaseous, liquid, and adsorbed phases (Fig. 4). The resonant structure at 2940 cm^{-1} corresponds to

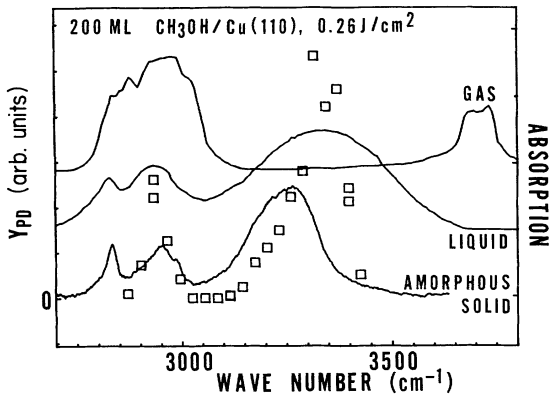

FIG. 4. Comparison of the Y_{PD} spectrum (laser fluence 0.26 J/cm^2) of an amorphous methanol film (90 K) with the ir spectra of various phases of methanol (the liquid- and gas-phase spectra are reproduced from Fig. 1 of Ref. 61).

excitation of the CH_{3a} vibration of methanol. It is worth noting that this CH_{3a} ir-absorption band does not shift significantly upon phase transition (solid-liquid-gaseous) and that the position of the CH_{3a} ir bands corresponds exactly to that of the CH_{3a} resonant structure. The second resonant structure at $\sim$3320 cm^{-1} corresponds to the excitation of the OH vibration. However, the maximum of this resonant structure is blueshifted versus the OH ir-absorption band of the amorphous methanol solid phase. This resonant-structure position corresponds to the center of the liquid methanol OH ir band. The position of this OH resonant structure is therefore a strong indication of the role played by the methanol liquid phase in the photodesorption process.

The evolution of Y_{PD} as a function of the laser fluence (F), for the same film and in the case of the resonant excitation of the OH vibration (laser-beam frequency 3317 cm^{-1}), is shown in Fig. 5. Because we were able to measure a five-order-of-magnitude change in Y_{PD}, the data are represented along both semilogarithmic and linear scales. We observe an initial linear evolution of $\log_{10}(Y_{PD})$ with the fluence, which then slowly saturates at higher fluence values. When the Y_{PD} evolution is presented on a linear scale, we observe an apparent threshold behavior at about 0.25 J/cm^2. Clearly, this threshold behavior, which was generally observed in the photodesorption experiments listed in Table I, is a representation artifact because the threshold value depends on mass-spectrometer sensitivity and the dynamical range of the Y_{PD} measurement. An apparent threshold may also be observed in the semilogarithmic representation. The $\log_{10}(Y_{PD})$ value increases for fluences higher than 0.05 J/cm^2 and stays nearly equal to zero below this value. This behavior, which can be better observed in Fig. 7, is due to the background detection, which limits the minimum value of Y_{PD} to one to three ions per window, depending on experimental conditions, therefore limiting the minimum value of $\log_{10}(Y_{PD})$ to 0–0.5, respectively.

Because of the nonlinear character of the Y_{PD} evolution as a function of the fluence, we expect an evolution of the relative importance of the resonant structures in the Y_{PD} spectra, as a function of the laser fluence. This is clearly demonstrated by the spectra presented in Fig. 6. In the first spectrum, measured at low fluence, the contrast between the two resonant-structure intensities is so high that the first one disappears in front of the second. The two structure intensities equalize as the fluence increases. This demonstrates that it is dangerous to infer a particular orientation of the adsorbed molecules from the relative importance of the resonant structures in the Y_{PD} spectrum, assuming that the latter can directly be compared to the adsorbate ir spectrum, as has been done for the system $C_4H_{10}/Al_2O_3(11\bar{2}0)$.[17,18] In Refs. 17 and 18, the differences in contrast between the resonant structures of the Y_{PD} spectrum and the ir-absorption bands of solid C_4H_{10} may, most probably, be a consequence of the nonlinear character of the photodesorption process.

The evolution of $\log_{10}(Y_{PD})$ as a function of fluence is compared for two different coverage values in Fig. 7. Here, again, the laser-beam frequency is tuned in resonance with the OH vibration. A similar qualitative evo-

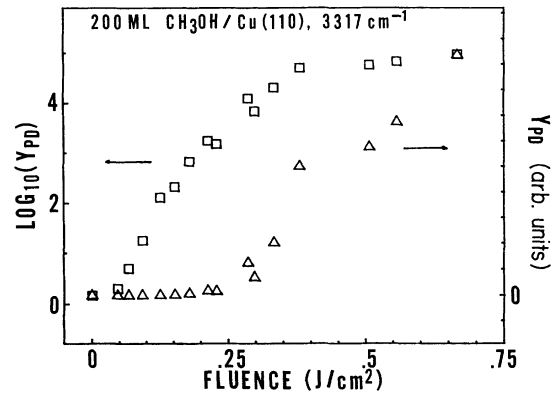

FIG. 5. Evolution of Y_{PD} as a function of the laser fluence while the laser frequency (3317 cm^{-1}) is tuned in resonance with the OH vibration. The data are represented along both a linear and a semilogarithmic scale.

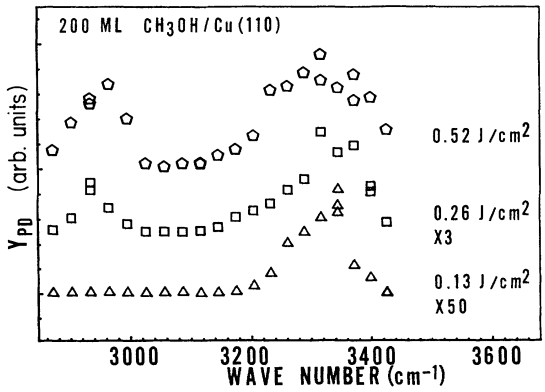

FIG. 6. Evolution of the Y_{PD} spectrum of an amorphous methanol film, as a function of the laser fluence.

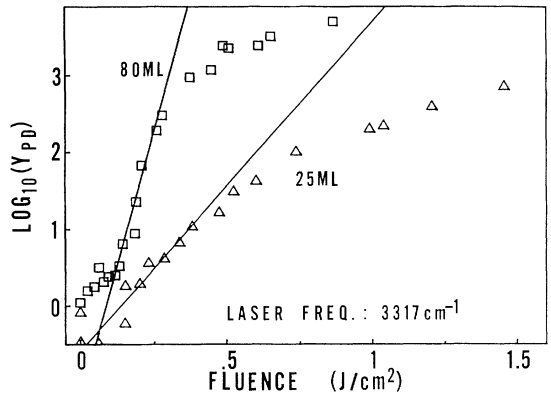

FIG. 7. Evolution of $\log_{10}(Y_{PD})$ vs the fluence, for two coverage values. The laser frequency is tuned in resonance with the OH vibration. In order to estimate the initial slopes, $\partial \log_{10}(Y_{PD})/\partial F_{init}$, a straight line is fitted on the first few data points above the detection threshold of $\log_{10}(Y_{PD})$. This threshold is equal to 0.5 and 0.1 for the coverage values of 80 and 25 ML, respectively.

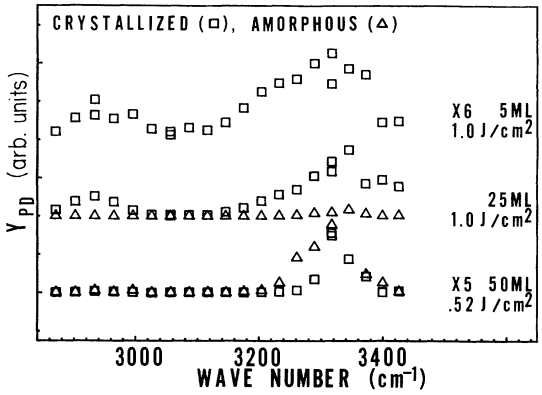

FIG. 9. Comparison of the Y_{PD} spectra of crystallized and amorphous methanol films for different coverage values. The fluence used to measure the two Y_{PD} spectra and the amplification factor are quoted on the right-hand side of the graph for each coverage value, respectively.

lution for both curves is observed. An estimate of the initial slope of the curves can be obtained by fitting the first few data points appearing above the detection threshold with a straight line using the least-squares method. Because of the dispersion of the data points, the measurement of this initial slope, $\partial \log_{10}(Y_{PD})/\partial F_{init}$, is rather inaccurate. Nevertheless, this slope clearly decreases with decreasing coverage values. All the measurements of these initial slopes, $\partial \log_{10}(Y_{PD})/\partial F_{init}$, for different coverages and for two laser frequencies (2933 and 3317 cm^{-1}) corresponding to the excitation of the CH_{3a} and OH vibrations, respectively, are presented in Fig. 8. Despite the data-point dispersion, the measurements appear to be in accordance with a hypothetical initial linear evolution of this slope, $\partial \log(Y_{PD})/\partial F_{init}$, with the coverage value. The slope saturates for coverage values above ~300 ML, for both laser frequencies. Hence, above 300 ML, Y_{PD}, at low fluences, no longer depends on adsorbate thickness. This gives the limit between the photodesorption and photoablation regimes; in the latter, Y_{PD} no longer depends on the nature of the substrate or the coverage. The independence of the photoablation yield versus the nature of the substrate was not tested in our experiment.

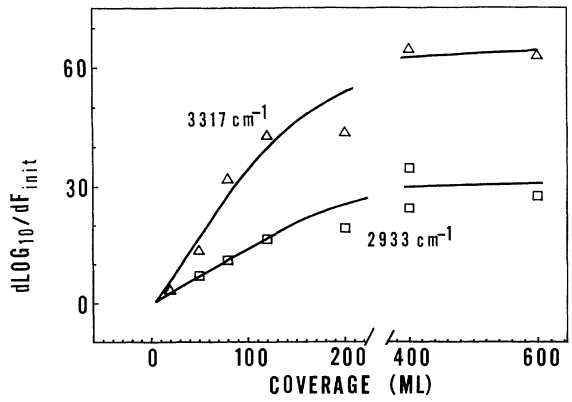

FIG. 8. Evolution of the initial slope, $\partial \log_{10}(Y_{PD})/\partial F_{init}$, as a function of the coverage and for two laser frequencies, 3317 and 2933 cm^{-1}, corresponding to the resonant excitation of the OH and CH_{3a} vibrations, respectively.

We also measured the evolution of Y_{PD} as a function of the substrate temperature from 90 to 130 K, the maximum temperature value being limited by the desorption of the multilayer phase. At coverages higher than 50 ML, no significant change of Y_{PD} versus the surface temperature was observed. In contrast, for lower coverages, an initial surface-temperature increase of 40 K was accompanied by an increase of Y_{PD}, which might be as high as two orders of magnitude for coverages below 10 ML. In fact, this drastic increase appears to be irreversible upon recooling the substrate to 90 K, and it is attributed to the crystallization of the methanol films. The Y_{PD} spectra of amorphous and crystallized films are compared in Fig. 9. Both spectra are similar for a 50-ML thickness. The increase of Y_{PD} for the crystallized thin films is readily observed for a thickness of 25 ML. For a 5-ML-coverage value, no Y_{PD} spectrum of the amorphous film could be measured because Y_{PD}, for our maximum achievable fluence, was below the signal generated by the background detection. On the other hand, the spectrum of a crystallized, 5-ML film could easily be recorded.

V. DISCUSSION

In the theoretical investigations of the photodesorption mechanisms due to the *elastic or inelastic tunneling*, the molecules are considered to interact individually with the laser beam and substrate. Therefore, Y_{PD} is expected to evolve linearly with the coverage. Both the fact that we performed photodesorption from multilayer adsorbates and the fact that we observed supralinear dependence of Y_{PD} versus coverage preclude the use of these models for interpretation of our experimental data. Both the models of *accumulation of the energy in the adbond vibration* or

the *destabilization of a surface vibrational mode* may be considered as intermediate between the above quantum photodesorption mechanisms and that implying a complete thermalization of the energy absorbed from the ir beam *(resonant heating)*.

In fact, the initial exponential evolution of Y_{PD} with fluence suggests the thermal nature of the photodesorption mechanism. Furthermore, both the supralinear evolution of Y_{PD} and the evolution of the slope, $\partial \log_{10}(Y_{PD})/\partial F_{init}$, with coverage, indicate the collective nature of the photodesorption process. The hypothesis of ir energy thermalization is also reinforced by measurements of vibrational excitation lifetimes of the high-frequency modes of organic molecules in liquid,[67] solid $(CH_2)_n$,[68] C_6H_6,[69] or adsorbed $(CH_2)_{16}CH_3/Ag$ (Ref. 70) and $CH_3S/Ag(111)$ (Ref. 71) phases. Indeed, the reported relaxation times are in the range 1–150 ps, which is at least two orders of magnitude smaller than the laser-pulse duration used in our experiment (~ 15 ns). These observations favor the interpretation of our results in the framework of the thermal photodesorption mechanism due to the *resonant heating* of the substrate. Within that model, the energy absorbed from the ir laser beam is supposed to degrade rapidly into heat, which dissipates into the substrate, causing a transient temperature increase of the substrate surface region. The latter provokes the thermal desorption of the adsorbate.

In order to obtain a quantitative interpretation, we have developed the following simple numerical model of the methanol photodesorption process. The first step is the evaluation of the laser-fluence fraction that is effectively absorbed and transmitted to the substrate. A first part of the ir beam is directly absorbed by the substrate due to its imperfect reflectivity. The corresponding *direct-absorption coefficient* is frequency independent in the frequency tunability range of the ir laser beam. It is computed, using the Fresnel formalism,[72] to be equal to 4.6% for the ir laser beam incidence angle and polarization condition adopted in our experiment (copper dielectric constant at 3000 cm^{-1}: $-500+i80$, Ref. 73). A second part of the ir beam is absorbed by the adsorbate. The corresponding *resonant-absorption coefficient* is strongly frequency dependent, and can be estimated from our IRAS measurements to be $\sim 0.3\%$ per adsorbed monolayer when the laser frequency is in resonance with the CH_{3a} vibration. This value is surely overestimated since the incidence angle of the ir beam emerging from the ir spectrometer ($\sim 84°$) is higher than that of the laser beam (73°). Therefore, the total fluence absorbed from the ir beam (F_t) as a function of the laser fluence (F) is given by the following equation when the CH_{3a} vibration is resonantly excited (laser wave number 2933 cm^{-1}) and the coverage is low:

$$F_t = F(4.6\% + (\approx 0.3\%/\mathrm{ML})\Theta) \ . \tag{2}$$

Thereafter, the substrate temperature evolution may be computed by solving the diffusion equation of heat into the solid. This problem was first solved by Bechtel,[74] who demonstrated that the lateral diffusion of the heat may be neglected for a laser-pulse duration of a few tens of nanoseconds. Within that approximation, and adopting the boundary conditions corresponding to the surface generation of heat,[43,74] the surface-temperature evolution in the laser spot, across which the irradiance is homogeneous, is given by

$$T(t) = 90\ \mathrm{K} + \frac{F_t}{(\tau\lambda\rho C\sqrt{2})^{1/2}} \times e^{-(t^2/2\tau^2)} D_{-1/2}(-\sqrt{2}(t/\tau)) \ , \tag{3}$$

where τ is the FWHM of the Gaussian laser-pulse temporal profile (15 ns). λ, ρ, and C are the heat conductivity, the density, and the specific heat of the substrate, respectively ($\lambda = 483\ \mathrm{W\,m^{-1}\,K^{-1}}/10^4$, $\rho = 8.93\times 10^3\ \mathrm{kg\,m^{-3}}$, $C = 255\ \mathrm{J\,kg^{-1}\,K^{-1}}$) (Ref. 75, p. D189). $D_{1/2}(\cdots)$ is the parabolic cylinder function.[76]

In expression (3), 90 K is the initial surface temperature. The second term on the right-hand side gives the temperature increase, proportional to the laser fluence.

Y_{PD} can be evaluated by integrating the desorption rate of the adsorbate along the temperature time profile given by (3). Because the adsorbate is supposed to melt during the photodesorption process, we adopt the desorption rate corresponding to the adsorbate vaporization. The latter is deduced from the kinetic theory of gases:[77]

$$\frac{d\Theta}{dt} = \frac{\text{vapor pressure at temperature } T}{(\text{monolayer density})\,[2\pi m_m (R/N_A)T]^{1/2}} \ , \tag{4}$$

where m_m and N_A are the molecular weight of methanol and Avogadro's number, respectively.

From the methanol-vapor pressure-temperature dependence given in the literature we obtain

$$\frac{d\Theta}{dt} = \left[\frac{6.24\times 10^{15}}{\sqrt{T}}\right] \times \exp\{-[(39.3\ \mathrm{kJ/mol})/RT]\}\ \ \mathrm{ML\,s^{-1}} \ . \tag{5}$$

Finally, in order to obtain a quantitative comparison between Y_{PD} estimated within this numerical model and the value determined experimentally, a calibration of the mass spectrometer must be obtained. This is achieved by dividing the integrated mass-spectrometer signal due to a 1-ML desorption during a TDS run by the ratio of the surfaces investigated by TDS and Y_{PD} spectroscopies. Hence, the photodesorption of 1 ML of methanol from the laser-spot surface could be estimated to correspond to a Y_{PD} signal of $\sim 7\times 10^2$ ions, in Figs. 5, 7, 8, and 11. This calibration is surely approximate since we have neglected the differences in speed and angular distribution between the photodesorbed molecules and those desorbing during a TDS run.

The numerical model that we have presented above has the advantage of simplicity. All the parameters needed for evaluating the photodesorption experimental signal are known or can be estimated. The model is indeed rather unrefined, since we neglected, among other things, the variation of the thermal properties of copper as a function of its temperature and the energy needed to

heat, melt, and vaporize the adsorbate. The latter is definitely below 10^2 kJ/mol; that is, below 5 mJ/cm^2 for the complete photodesorption of a 50-ML film. This value is at least one order of magnitude smaller than F_t, which indeed indicates the efficiency of the energy dissipation into the substrate, the energy used to break the adbonds being negligible in comparison to that used to heat the substrate. The numerical model also neglects the adsorbed phase change during the photodesorption process. The methanol melting should be accompanied by a change in the *resonant-absorption coefficient*. Therefore, this coefficient must be considered as representative of the average ir property of the adsorbate during the photodesorption process. This numerical analysis will also be limited to the case of the resonant excitation of the CH_{3a} vibration (laser wave number 2933 cm^{-1}), the case of the OH vibration excitation being more complicated since the corresponding ir-absorption band shifts considerably during the adsorbate melting. This model is only valid in the limit of low fluence, where the amount of photodesorbed molecules remains negligible in comparison to the total adsorbate thickness. We effectively neglected the *resonant-absorption coefficient* modification during the irradiation due to the adsorbate depopulation. Hence, the model is not designed to describe the saturation of $\log_{10}(Y_{PD})$ versus F. As already mentioned by Chuang *et al.*,[9,10,23,24] this saturation may not necessarily be a consequence of the adsorbate depopulation. Nevertheless, the above approximate calibration of the Y_{PD} measurement indicates that, in our case, significant depopulation occurs. For example, in Fig. 5 the $\log_{10}(Y_{PD})$ saturation value of 5 corresponds to photodesorption of about 1.4×10^2 ML [$(10^5$ ions$)/(7\times10^2$ ions ML^{-1})], which is close to the exposure value of 200 ML. The model is also limited to the case of thin adsorbates. When the thickness increases, the *resonant-absorption coefficient* dependence versus coverage departs from the linear relationship assumed in Eq. (2). Furthermore, the hypothesis of a homogeneous adsorbate temperature equal to that of the underlying substrate subsurface becomes more questionable as the adsorbate thickness increases. Therefore, the model will not allow us to describe the saturation of the slope, $\partial\log_{10}(Y_{PD})/\partial F_{init}$, observed in Fig. 8 for coverages higher than 200 ML. Finally, we gave ourselves the freedom to adjust the *resonant-absorption coefficient* slightly in order to obtain the best fit of the theoretical curves with the experimental ones.

The results of the numerical analysis are shown in Figs. 10 and 11. The best correspondence between the theoretical and experimental curves is achieved with a *resonant-absorption coefficient* of 0.24%/ML. The similitude between that value and the one estimated by ir spectroscopy (0.3%/ML) strongly indicates the validity of the proposed photodesorption mechanism. The computed surface-temperature evolution, for a typical set of experimental parameters (50 ML, $F=0.5$ J/cm^2, laser frequency of 2933 cm^{-1}) is presented in Fig. 10. Under these conditions, the surface temperature rises above 250 K, definitely above the melting point of methanol, which lies at 180 K (Ref. 75, p. C412). This clearly supports the hypothesis that methanol melts during the photodesorption process. The experimental and theoretical evolutions of Y_{PD} as a function of fluence and for two coverage values (80 and 50 ML) are compared in Fig. 11. A background detection of 2 pulses per window has been added to the numerically evaluated Y_{PD}. This limits the minimum value of the theoretical $\log_{10}(Y_{PD})$ to ~0.3.

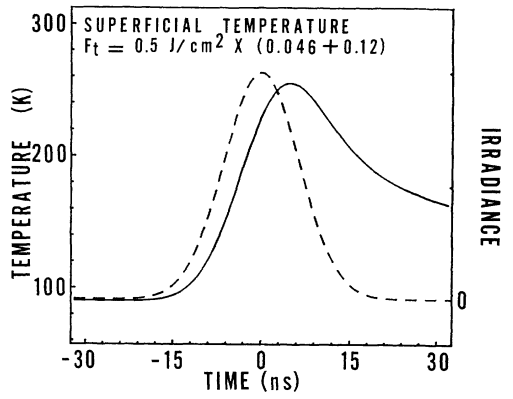

FIG. 10. Temporal evolution of the surface temperature according to Eq. (3) and for a typical set of experimental parameters: 50-ML-thick adsorbate, laser frequency in resonance with the CH_{3a} vibration (2933 cm^{-1}), fluence of 0.5 J/cm^2, and resonant-absorption coefficient of 0.24% per adsorbed monolayer. Solid line, surface temperature; dashed line, temporal profile of the laser pulse.

In the numerical model, the decrease of the coverage value simply induces the decrease of the *resonant-absorption coefficient* and, correspondingly, of the ratio F_t/F. This corresponds, graphically, to a dilation of the fluence axis or to a rightward shift of the curves in Fig. 11. This behavior is well verified for the experimental

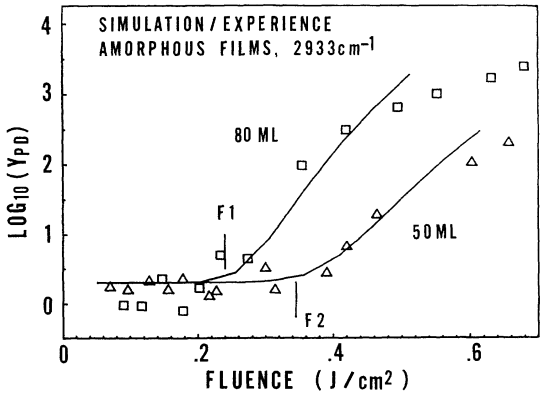

FIG. 11. Comparison between the calculated and experimental evolution of Y_{PD} as a function of the laser fluence for two coverage values. The laser frequency is in resonance with the CH_{3a} vibration (2933 cm^{-1}). F_1 and F_2 correspond to the theoretical fluence thresholds for the adsorbate melting.

and theoretical curves. It is also worth noting that this rightward shift is accompanied by a decrease of the initial slope, $\partial \log_{10}(Y_{PD})/\partial F_{init}$. This is, indeed, in agreement with our observation of the linear evolution of that slope with coverage, as observed in Fig. 8. Finally, we have denoted—by F_1 and F_2—the fluences that provoke a maximum surface temperature just reaching the methanol melting point (180 K), for the 80- and 50-ML adsorbate, respectively. For both coverages, we observe that these thresholds must be overstepped in order to render Y_{PD} detectable. This numerical modelization is therefore in agreement with our experimental observation of the correspondence between the Y_{PD} spectra and the ir spectrum of liquid methanol, for all the experimental conditions where Y_{PD} could be measured.

Nevertheless, one should not put too much emphasis on the accuracy of the various parameters used in this numerical analysis. The influences of the parameter inaccuracies on the calculated $\log_{10}(Y_{PD})$ curves in Fig. 11 have been discussed elsewhere.[78] It was shown, for example, than an overestimation of the Y_{PD} calibration value by a factor as great as 3 does not significantly displace the calculated curve, or that it may be compensated by a similar underestimation of the frequency factor of the desorption kinetics. Similarly, a slight error in the activation energy for desorption is readily compensated by accordingly modifying the *resonant-absorption coefficient.* Clearly, the result of our modelization is the ability to interpret quantitatively the experimental data, while adopting a reasonable set of parameter values.

The numerical model also "foresees" a Y_{PD} increase of a factor 2–4, depending on the fluence, as the substrate temperature varies from 90 to 120 K. This is definitely obscured by the irreversible two-order-of-magnitude Y_{PD} increase due to the crystallization of the adsorbate when the latter is thinner than 50 ML. For thicker films, this theoretical increase has the same magnitude as the pulse-to-pulse variation of Y_{PD} around its average value. This clearly renders the observation of the "small," theoretically foreseen substrate temperature dependence of Y_{PD} precarious.

Finally, we tentatively assign the irreversible drastic Y_{PD} increase upon adsorbate crystallization to its morphology change. Indeed, this increase cannot be accounted for by the small ir-absorbance difference between the amorphous and crystallized methanol films, because in that case we would expect to observe this Y_{PD} increase for both thin (<50 ML) and thick (>50 ML) methanol films, in clear contradiction with the experimental observations. Therefore, we tentatively propose that this increase might be a consequence of the formation of aggregates upon thin-film crystallization. Packing of methanol into crystallites was already proposed in our previous IRAS investigation.[59] If the crystallite sizes are greater than the average film thickness, crystallization of thin films should provoke an increase in film corrugation. Because of the strong nonlinear dependence of Y_{PD} on the "local" adsorbate thickness, this may entail a substantial increase of Y_{PD}. Furthermore, as the film becomes much thicker than the crystallite size, polycrystallization would no longer modify the adsorbate corrugation, explaining the absence of Y_{PD} increase upon thick-film annealing.

VI. CONCLUSIONS

In this work we demonstrate the resonant character of the ir photodesorption process of CH_3OH from Cu(110). Two remarkable features are observed. First, the OH resonant-structure position of the Y_{PD} spectra is blue-shifted in comparison to the OH ir-absorption band of the solid adsorbed phase of methanol, and also corresponds to the center of the OH band of liquid methanol, indicating that desorption occurs mostly after the film has melted. Second, the relative intensity of the Y_{PD} spectrum resonant structures depends on fluence, which is a consequence of the nonlinear character of this spectrodynamics.

The experimental results could be quantitatively analyzed in the framework of the photodesorption mechanism due to the resonant heating of the substrate. We emphasize the fact that this agreement is achieved by adjusting only the adsorbate ir absorbance to a value remarkably similar to that obtained by our IRAS measurements, while all the other parameters could either be determined experimentally or taken from the literature. However, this numerical analysis was limited to the case of the resonant excitation of the CH_{3a} vibration, and for weak-fluence values, where the number of photodesorbed molecules is small compared to the total adsorbate thickness. Moreover, a number of other simplifying hypotheses had to be made in order to render the calculation tractable. We feel that a more accurate model should first take into account the pulse-to-pulse fluctuation of the measured Y_{PD}, which may be a consequence of the adsorbate statistical corrugations.

As testified to by the linear evolution of the slope, $\partial \log_{10}(Y_{PD})/\partial F_{init}$, with coverage, as presented in Fig. 8, the photodesorption mechanism due to substrate resonant heating appears to be operative from 25- to 200-ML-thick amorphous methanol films. Above this latter value, the saturation of the slope versus coverage indicates that the adsorbate vibrational energy transfer to the substrate becomes less relevant. The low-coverage range of the amorphous-film photodesorption investigation is limited by the maximum fluence available. The latter is not sufficient to obtain a detectable Y_{PD} below an amorphous-film thickness of ~ 10 ML.

The thermal nature of the photodesorption process was already proposed for various reactive systems such as $NH_3/Cu(100)$ (Ref. 24) or $C_4H_{10}/Al_2O_3(11\bar{2}0)$,[17] and was suggested by the lack of isotopic selectivity in the photodesorption process.[9,15–17,24] Clearly, our work demonstrates the possibility of foreseeing the efficiency of this photodesorption process from both the knowledge of the ir absorbance and the desorption kinetics of the adsorbate.

Finally, the observation of a nonthermal photodesorption process, resulting, for example, from the *elastic tunneling* to a desorption state, is one of the objectives of the ir photodesorption experiments. The experimental conditions that may favor this observation are those that

reduce the efficiency of the thermal process. These conditions are the decrease of the initial substrate temperature, which might be achieved by using liquid helium as a refrigerant, and the decrease of the adsorbate coverage, which would reduce the fraction of fluence transmitted to the substrate, but would necessitate higher fluences in order to keep Y_{PD} detectable. The use of picosecond ir pulses, the duration of which may be smaller than the organic adsorbate vibrational mode relaxation times, also offers better chances for the observation of nonthermal photodesorption pathways. We plan to pursue our investigations in that direction.

ACKNOWLEDGMENTS

We thank M. Renier, F. Rase, and V. Froidbise for their contributions to the setting up of the experiment. The optical parametric oscillator was developed by Dr. M. Bucchia. This work was funded by the Belgian Program on Interuniversity Attraction Poles and by the Fonds National pour la Recherche Scientifique (FNRS, Brussels). The authors acknowledge the use of the Namur Scientific Computing Facility, a common project between the FNRS, IBM-Belgium, and the Facultés Universitaires Notre Dame de la Paix.

[1] *Lasers and Chemical Changes,* edited by A. B. Shanl, Y. Haas, K. L. Kompa, and R. D. Levine (Springer-Verlag, Berlin, 1981).

[2] A. M. Ronn, in *Applications of Lasers to Chemical Problems,* edited by T. R. Evans (Wiley, New York, 1982), pp. 225–271.

[3] W. C. Danen and J. C. Janz, in *Laser Induced Chemical Processes,* edited by J. I. Steinfeld (Plenum, New York, 1981), pp. 45–164.

[4] K. S. Gochelaskvili, N. V. Karlov, A. I. Orchenkov, and A. N. Orlov, Zh. Eksp. Teor. Fiz. **70**, 531 (1976) [Sov. Phys.—JETP **43**, 274 (1976)].

[5] M. E. Umstead and M. C. Lin, J. Phys. Chem. **82**, 2047 (1978).

[6] C. T. Lin and T. D. Z. Atvars, J. Chem. Phys. **68**, 4233 (1978).

[7] T. J. Chuang, in *Vibrations at Surfaces,* edited by R. Caudano, J. M. Gilles, and A. A. Lucas (Plenum, New York, 1982), pp. 573–577.

[8] A. Peremans, J. Darville, and J.-M. Gilles. Bull. Soc. Roy. Sci. Liège **58**, 283 (1989).

[9] T. J. Chuang, J. Electron Spectrosc. Relat. Phenom. **29**, 125 (1983).

[10] T. J. Chuang, J. Chem. Phys. **76**, 3828 (1982).

[11] J. Heidberg, H. Stein, and E. Riehl, Phys. Rev. Lett. **49**, 666 (1982).

[12] J. Heidberg, H. Stein, E. Riehl, Z. Szilagyi, and H. Weiss, Surf. Sci. **158**, 553 (1985).

[13] J. Heidberg, H. Stein, and E. Riehl, Surf. Sci. **126**, 183 (1983).

[14] J. Heidberg, H. Stein, E. Riehl, and A. Nestmann, Z. Phys. Chem. **121**, 145 (1980).

[15] J. Heidberg, H. Stein, and H. Weiss, Surf. Sci. **184**, L431 (1987).

[16] J. Heidberg, K.-W. Stahmer, H. Stein, and H. Weiss, J. Elec. Spectrosc. **45**, 87 (1987).

[17] N. J. Tro, D. A. Arthur, and S. M. George, J. Chem. Phys. **90**, 3389 (1989).

[18] S. V. Benson, J. Schultz, B. A. Hooper, R. Crane, and J. M. J. Madey, Nucl. Instrum. Method Phys. Res. A **272**, 22 (1988).

[19] J. Heidberg and D. Hoge, J. Opt. Soc. Am. B **4**, 242 (1987).

[20] T. J. Chuang, H. Seki, and I. Hussla, Surf. Sci. **158**, 525 (1985).

[21] T. J. Chuang and H. Seki, Phys. Rev. Lett. **49**, 382 (1982).

[22] H. Seki and T. J. Chuang, Solid State Commun. **44**, 473 (1982).

[23] T. J. Chuang and I. Hussla, Phys. Rev. Lett. **52**, 2045 (1984).

[24] I. Hussla, H. Seki, T. J. Chuang, Z. W. Gortel, H. J. Kreuzer, and P. Piercy, Phys. Rev. B **32**, 3498 (1985).

[25] T. J. Chuang, J. Vac. Sci. Technol. B **3**, 1408 (1985).

[26] J. Heidberg, H. Stein, A. Nestmann, E. Hoefs, and I. Hussla, in *Laser-Solid Interaction and Laser Processing,* edited by S. D. Ferris, H. J. Leamy, and J. M. Poate, AIP Conf. Proc. No. 50 (AIP, New York, 1979), pp. 49–54.

[27] B. Schäfer and P. Hess, Chem. Phys. Lett. **105**, 563 (1984).

[28] B. Schäfer and P. Hess, Appl. Phys. B **37**, 197 (1985).

[29] M. Buck, B. Schäfer, and P. Hess, Surf. Sci. **161**, 245 (1985).

[30] M. Buck and P. Hess, J. Elec. Spectrosc. **45**, 237 (1987).

[31] M. Buck and P. Hess, in *Fundamentals of Beam-Solid Interactions and Transient Thermal Processing,* Materials Research Society Symposia Proceedings No. 100, edited by M. J. Aziz and L. E. Rehn (MRS, Pittsburgh, 1988), pp. 647–652.

[32] B. Schäfer, M. Buck, and P. Hess, Infrared Phys. **25**, 245 (1985).

[33] J. Heidberg, L. Langowski, G. Neubauer, and M. Folman, J. Electron. Spectrosc. Relat. Phenom. **45**, 249 (1987).

[34] J. Heidberg, C. Langowski, and C. Neubauer, Surf. Sci. **189/190**, 946 (1987).

[35] M. Buck and P. Hess, Chem. Phys. Lett. **158**, 486 (1989).

[36] H.-C. Chang and G. E. Ewing, Chem. Phys. **139**, 55 (1989).

[37] J. Heidberg and I. Hussla, J. Electron. Spectrosc. **29**, 105 (1983).

[38] I. Hussla and R. Viswanathan, J. Vac. Sci. Technol. B **3**, 1520 (1985).

[39] P. Hess, *Photoacoustic, Photothermal, and Photochemical Processes at Surfaces and in Thin Films,* edited by P. Hess, Topics in Current Physics Vol. 47 (Springer-Verlag, Berlin, pp. 55–87.

[40] M. S. Slutsky and T. F. George, J. Chem. Phys. **70**, 1231 (1979).

[41] A. C. Beri and T. F. George, J. Vac. Sci. Technol. B **3**, 1529 (1985).

[42] S. Van Smaalen, A. Peremans, H. F. Arnoldus, and T. F. George, Spectrochim. Acta **43A**, 201 (1987).

[43] A. Dereux, A. Peremans, J.-P. Vigneron, J. Darville, and J.-M. Gilles, J. Electron Spectrosc. Relat. Phenom. **45**, 261 (1987).

[44] D. Lucas and G. E. Ewing, Chem. Phys. **58**, 385 (1981).

[45] H. J. Kreuzer and D. N. Lowy, Chem. Phys. Lett. **78**, 50 (1981).

[46] Z. W. Gortel, H. J. Kreuzer, P. Piercy, and R. Teshima, Phys. Rev. B **27**, 5066 (1983).

[47] B. Fain, S. H. Lin, and Z. W. Gortel, Surf. Sci. **213**, 531 (1989).

[48] A. B. Ephraim, M. Folman, J. Heidberg, and N. Moiseyev, J. Chem. Phys. **89**, 3840 (1988).

[49] A. Peremans, J. Darville, J-M. Gilles, and T. F. George, Phys. Rev. B **35**, 2690 (1987).

[50] H. J. Kreuzer, Z. W. Cortel, and P. Piercy, J. Opt. Soc. Am. B **4**, 248 (1987).

[51] Z. W. Gortel, P. Piercy, R. Teshima, and K. J. Kreuzer, Surf. Sci. **165**, L12 (1986).

[52]Z. W. Gortel, P. Piercy, R. Teshima, and H. J. Kreuzer, Surf. Sci. **179**, 176 (1987).
[53]A. Peremans, J. Darville, and J.-M. Gilles, J. Electron Spectrosc. Relat. Phenom. **48**, 405 (1989).
[54]B. Fain, V. Fleurov, and S. H. Lin, Chem. Phys. **122**, 17 (1988).
[55]A. Peremans, M. Bucchia, J. Darville, and J.-M. Gilles, J. Electron Spectrosc. Relat. Phenom. **54/55**, 173 (1990).
[56]A. Peremans, F. Maseri, J. Darville, and J.-M. Gilles. Proc. SPIE **1204**, 808 (1990).
[57]I. E. Wachs and R. J. Madix, J. Catal. **53**, 208 (1978).
[58]B. A. Sexton, A. E. Hughes, and N. R. Avery, Surf. Sci. **155**, 366 (1985).
[59]A. Peremans, F. Maseri, J. Darville, and J.-M. Gilles, J. Vac. Sci. Technol. A **8**, 3224 (1990).
[60]K. J. Tauer and W. N. Lipscomb, Acta Crystallogr. **5**, 606 (1952).
[61]M. Falk and E. Whalley, J. Chem. Phys. **34**, 1554 (1961).
[62]A. B. Dempster and G. Zerbi, J. Chem. Phys. **54**, 3600 (1971).
[63]D. H. Ehlers, A. Spitzer, and H. Lüth, Surf. Sci. **160**, 57 (1985).
[64]M. A. Chesters and E. M. McCash, Spectrochim. Acta **43A**, 1625 (1987).
[65]R. J. Jakobsen, J. W. Brasch, and Y. Mikawa, J. Mol. Struc. **1**, 309 (1967).
[66]R. G. Greenler, J. Chem. Phys. **50**, 1963 (1969).
[67]James T. Yardley, *Introduction to Molecular Energy Transfer* (Academic, New York, 1980), pp. 186 and 187.
[68]H. Graener and A. Laubereau, Chem. Phys. Lett. **133**, 378 (1987).
[69]R. M. Hochstrasser, in *Time-Resolved Vibrational Spectroscopy,* edited by A. Laubereau and M. Stockburger, Springer Proceedings in Physics Vol. 4 (Springer-Verlag, Berlin, 1985), pp. 96–99.
[70]A. L. Harris and N. J. Levinos, J. Chem. Phys. **90**, 3878 (1989).
[71]A. L. Harris, L. Rothberg, L. H. Dubois, N. J. Levinos, and L. Dhar, Phys. Rev. Lett. **64**, 2086 (1990).
[72]*Classical Electrodynamics,* edited by J. D. Jackson (Wiley, New York, 1975).
[73]M. A. Ordal, R. J. Bell, R. W. Alexander, L. L. Long, and M. R. Querry, Appl. Opt. **24**, 4493 (1985).
[74]J. H. Bechtel, J. Appl. Phys. **46**, 1585 (1975).
[75]*CRC Handbook of Chemistry and Physics,* 61st ed., edited by R. C. Weast, and M. J. Astle (Chemical Rubber Co., Boca Raton, FL, 1980).
[76]*Handbook of Mathematical Functions,* edited by M. Abramowitz and I. A. Stegun (Dover, New York, 1972), pp. 295 and 685.
[77]*Treatise on Solid State Chemistry,* edited by N. B. Hannay (Plenum, New York, 1976), Vol. 6A, pp. 169–173.
[78]A. Peremans, Ph.D. thesis, Facultés Universitaires Notre Dame de la Paix, Namur, Belgium (1990) (unpublished).